J. Phys.: Condens. Matter 6 (1994) 9759–9772. Printed in the UK

Phase transitions in Ising square antiferromagnets with first- and second-neighbour interactions

J L Morán-López†, F Aguilera-Granja† and J M Sanchez‡

† Instituto de Física 'Manuel Sandoval Vallarta', Universidad Autónoma de San Luis Potosí, 78 000 San Luis Potosí, SLP, Mexico

‡ Center for Materials Science and Engineering, University of Texas, Austin, TX 78712-1063, USA

Received 19 April 1994

Abstract. The phase transitions occurring in the Ising square antiferromagnet with first- (J_1) and second- (J_2) nearest-neighbour interactions are studied using several mean-field approximations and for a wide range of $R = J_2/J_1$. The largest approximation used corresponds to a nine-point cluster approximation of the cluster variation method. In this case, the transition temperatures as a function of R are found to be in excellent agreement with those obtained by other methods. The mean-field approximations predict a first-order transition in the range $0.5 < R \lesssim 1.2$, where the critical exponents associated with the paramagnetic to superantiferromagnetic transition have been reported to vary continuously with R. In that range of R, the mean-field approximations also predict a crossover between two distinct instability temperatures, or spinodals, taking place immediately below the first-order transition. Mean-field results are also given for the magnetization m, the specific heat C_v, the magnetic susceptibility χ, the staggered susceptibility χ_s, and the pair correlation function σ_{ij} between i and j sites.

1. Introduction

Although the general properties of the Ising model on a square lattice with first- (J_1) and second- (J_2) neighbour interactions are relatively well known, several recent studies suggest a non-universal critical behaviour for values of $R = J_2/J_1 > 0.5$. This particular behaviour has motivated studies based on finite-size scaling [1], perturbation theory [2], low- [3] and high- [4] temperature expansions, Monte Carlo simulations [5–8] and, more recently, the cluster variation method (CVM) [9] and the coherent anomaly method (CAM) [10].

Since the thermodynamic properties of the model are independent of the sign of the J_1, we restrict our discussion to the case of antiferromagnetic nearest-neighbour interactions, i.e. $J_1 < 0$. For values of $R = J_2/J_1 < 0.5$ the ground state is the antiferromagnet (AF), consisting of two ferromagnetic interpenetrating sublattices. For $R > 0.5$, the ground state is an arrangement with superantiferromagnetic order (SAF). This phase can be described by alternate single ferromagnetic rows of opposite oriented spins (see figure 1). Of special interest is the point $R = 0.5$ for which the system is highly degenerate and remains disordered at all finite temperatures. Recently it has been suggested that for $R = 0.5$ the system behaves as the one-dimensional Ising chain [11]. As it is shown below this behaviour is also observed in our calculations.

It has been proposed that with the inclusion of second neighbour interactions, the system displays non-universal critical behaviour. For example, finite-size scaling studies [1] of Baxter's model indicated that the critical exponents vary continuously not only in

0953-8984/94/459759+14$19.50

the case where four-spin interactions are included but also in the case in which the Ising Hamiltonian contains only first- and second-neighbour pair interactions. A similar behaviour was obtained by perturbation theory [2] for systems with ferromagnetic J_1, antiferromagnetic J_2, and small values of $-R^{-1}$. Furthermore, based on low-temperature series expansion studies, Wu [3] concluded that systems with $R \neq 0$ do not belong to the Ising class. Later Oitmaa [4] extended the analysis to high temperatures and found that universality breaks down for $R > 0.5$. More recently, Tanaka *et al* [10] have used the CAM together with a simplified version of the CVM in order to estimate the critical exponents. However, the CVM predicts a first-order transition in the region where the exponents are seen to vary with R and, thus, the applicability of the CAM needs careful re-examination [9].

The model has been also a subject of several studies by means of Monte Carlo simulations [5–8]. In these studies the critical exponents also show a non-universal behaviour for $R > 0.5$, but the critical properties approach the two-dimensional Ising behaviour for large R. On the other hand, for $R < 0.5$ critical behaviour is Ising-like, i.e. only for a range of values of $R > 0.5$ do the exponents seem to be non-universal.

The finite-temperature behaviour has been also studied in detail in the neighbourhood of $R = 0.5$. The possible existence of a multicritical point separating the ferromagnetic (or AF) and SAF states at finite temperatures at $R = 0.5$ was ruled out by exact calculations; a disorder line was obtained for $R < 0.5$ and shown to approach $R = 0.5$ only in the limit of $T \to 0$ [12]. More recently, it has been shown that the model can be mapped onto an Ising chain in a transverse field [11]. This approximation is valid only for values of R close to 0.5 and, due to field inversion symmetry, the magnetic properties are symmetrical with respect to that value. The critical exponents obtained within this approach are of the Ising universality class.

An additional feature of the Ising systems with ferromagnetic nearest neighbours and antiferromagnetic next-nearest-neighbour interactions, or with antiferromagnetic J_1 in the range $0 < R < 0.5$, is the behaviour of the spin–spin pair correlation functions. In this case, a disorder temperature T_D has been defined in the paramagnetic state as the temperature at which the pair correlations for infinite distance change sign [13].

Here we describe the results of a systematic study of the Lenz–Ising model with first- and second-neighbour interactions using the CVM [14]. The Hamiltonian is solved in the square, five-, eight-, and nine-point approximations and the thermodynamic properties predicted by the mean field approximations are determined. We studied the phase transitions as a function of the interactions ratio R. As has been pointed out before, the transitions for values of $0.5 < R < 1.2$ are found to be of first order. However, as the cluster size increases and the level of the mean field approximation improves, the line of first-order transitions approaches two distinct critical lines (spinodals), corresponding to two different instabilities, depending on the value of R. A crossover between these two instabilities is found to take place for $R \approx 0.60$–0.65.

Although the CVM by itself is not expected to resolve the issue of the true critical behaviour of the system, the method can be used in conjunction with the CAM to produce reliable estimates of critical exponents. Here we present a full characterization of the mean field CVM solutions, which is required for future applications of the CAM. Furthermore, the CVM provides accurate estimates of the transition temperatures and of the correlation spectrum near the critical point. In particular, in the nine-point approximation used here, one can calculate the pair correlations up to fifth neighbours. In section 2 we present briefly the model and method of solution. The results and conclusions are presented in section 3 and a brief summary is given in section 4.

2. Model and method

The CVM provides a hierarchy of approximations to the configurational entropy of lattice systems. The simplest level of this method is equivalent to the Bragg–Williams (BW) or mean-field approximation [15]; in this approximation all the spin correlations are neglected. The next level of the CVM takes into account the spin correlation between first-neighbour pairs and is equivalent to the approximation developed independently by Bethe, Peierls and Guggenheim [16].

One can continue this series of approximations and consider larger and larger clusters with the consequent improvement in the description of the thermodynamic properties of the system. The exact solution would be achieved by considering an infinite cluster. However, as it is shown below, by using relatively small clusters that contain the topology of the lattice, one can obtain a reasonable description of thermodynamic properties. In the particular case of the square lattice, the smallest cluster that contains the information of the lattice topology is the square. The approximation based on the square is equivalent to the one worked out by Kramers and Wannier [17].

We solved the Hamiltonian using four, five, eight, and nine points as basic clusters. In the highest approximation, nine spin correlations, as well as the correlations in the smaller subclusters, are taken into account. The highest approximation used to study the Ising square lattice is the one based on nine-point clusters and it has been applied recently to the study of oxygen ordering in ceramic superconductors [18].

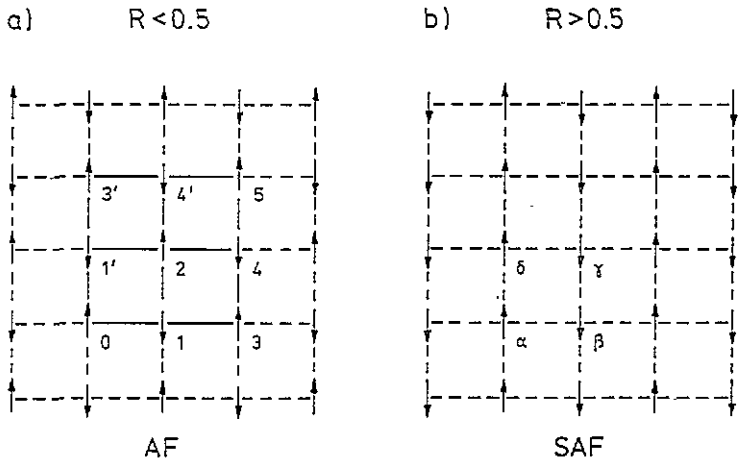

Figure 1. The ground state antiferromagnetic arrangements on the square lattice for $R = J_2/J_1 < 0.5$ (antiferromagnetic) and $R > 0.5$ (superantiferromagnetic). (a) The various neighbours to site zero in the nine-point cluster and (b) the four sublattices necessary to describe the magnetic order.

The model considered is illustrated in figure 1. The AF and the SAF states at $T = 0$ are shown in figure 1(a) and (b), respectively. We assume a spin at each lattice site that interacts with its first and second neighbours. Thus the Hamiltonian describing the system is

$$\mathcal{H} = -J_1 \sum_{(i,j)} \sigma_i \sigma_j - J_2 \sum_{(i,j)'} \sigma_i \sigma_j - H \sum_i \sigma_i \tag{1}$$

where (i, j) and $(i, j)'$ refer to first and second neighbours, $\sigma_i = \pm 1$, and H is a constant magnetic field.

To describe the two antiferromagnetic phases, the square lattice has to be subdivided into four interpenetrating sublattices: α, β, γ, and δ (see figure 1). The magnetization at each sublattice is defined by

$$M_\nu = \frac{4}{N} \sum_{i \in \nu} \langle \sigma_i \rangle \tag{2}$$

where N is the total number of lattice sites. The magnetizations in the AF and SAF states are given in terms of the sublattice magnetizations by

$$M_{\mathrm{AF}} = [M_\alpha + M_\gamma - (M_\beta + M_\delta)]/4 \tag{3a}$$

$$M_{\mathrm{SAF}} = [M_\alpha + M_\delta - (M_\beta + M_\gamma)]/4 \tag{3b}$$

and the specific heat and the magnetic susceptibilities are given by

$$C_\nu = \left(\frac{\partial U}{\partial T}\right)_{H=0} \tag{4a}$$

$$\chi_{\mathrm{m}} = \left(\frac{\partial M}{\partial H}\right)_{H=0} \tag{4b}$$

$$\chi_s = \left(\frac{\partial M_\nu}{\partial H_s}\right)_{H_s=0} \tag{4c}$$

where H_s is the staggered magnetic field.

The equilibrium properties of the system at finite temperatures are obtained by using a generalization of the self-consistent mean-field approximation [19]. This formulation is fully equivalent to the cluster variation method and allows us to treat large clusters in a simpler and more efficient computational manner.

3. Results

3.1. The case $R = 0$

To illustrate the accuracy of our calculations we present first the results obtained in the absence of second-neighbour interactions. In figure 2(a) we show the temperature dependence of the magnetization as obtained in the Wannier–Kramers approximation (four points), the nine-point approximation, and Yang's exact result. In this figure the temperature has been scaled to the critical temperature T_c of each approximation. We notice that the nine-point approximation reproduces well the exact result over most of the temperature range. In figure 2(b) we present the results for the temperature dependence of the specific heat C_ν as obtained in the two cluster approximations and compare them with the exact result.

It is worth noticing that the critical temperature $(k_{\mathrm{B}}T_c/J_1)$ is 4, 2.425 75 and 2.346 29 as obtained in the BW, square and nine-point approximations respectively; i.e. 76.3%, 6.9%, and 3% higher than the exact value (2.269 18). Thus the accuracy of the approximation increases relatively quickly with the cluster size. For further reference, and to compare with

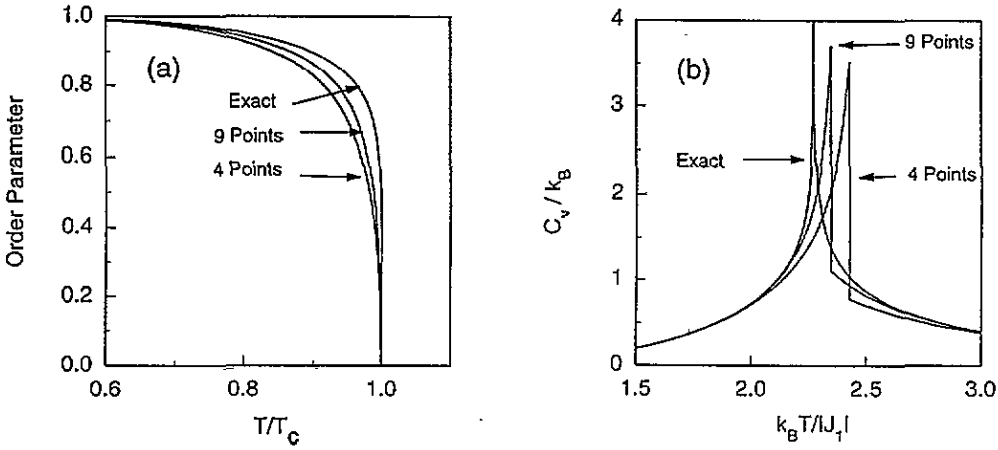

Figure 2. (a) The temperature dependence of the magnetization in a square ferromagnet as obtained in the square and nine-point approximations of the CVM, and the exact result. The temperature is scaled to the corresponding critical temperature. (b) The temperature dependence of the specific heat for the same approximations and the exact result.

the $R > 0$ cases, the temperature dependence of the order parameter (average magnetization), the specific heat C_v, the magnetic susceptibility χ_m, and the staggered susceptibility χ_s, as obtained in the nine-point cluster approximation, are presented in figure 3.

In the nine-point approximation, the spin–spin correlations are defined up to fifth neighbours. In figure 1(a) the nine-point cluster is shown and the various neighbours to the site 0 are marked. In contrast to the SAF phase, in the AF state the primed and non-primed neighbours are equivalent. We show in figure 4 our results for the spin–spin correlations $\langle\sigma\sigma\rangle_{0j}$, $(j=1,...,5)$ above T_c. The correlations between first and fourth neighbours are antiferromagnetic (less than zero) and those between second, third, and fifth neighbour are ferromagnetic (greater than zero). They decay monotonically to zero as a function of the spin separation and/or the temperature. At high temperatures only the first-neighbour spin correlation has an appreciable value.

3.2. The antiferromagnetic phase $0 < R < 0.5$

With the inclusion of antiferromagnetic coupling between second neighbours, a competition is set up between the two interactions. Now the ferromagnetic correlations between second neighbours are in conflict with their interaction. For values of $R < 0.5$ the ground state is the antiferromagnet and, due to the competing interactions, the transition temperature is reduced as J_2 increases.

We show in figure 5 the results for the order parameter (average magnetization), the specific heat C_v, the magnetic susceptibility χ_m and the staggered susceptibility χ_s for $R = 0.2$ and 0.4. The results for $R = 0$ are also included for comparison. One can notice that the effect of J_2 is to increase the order near T_c (see figure 5(a)). Also observed is the respective narrowing and widening of the specific heat and of the staggered magnetic susceptibility. The phase transitions in this range of interactions are of second order.

More interesting is the behaviour of the spin–spin correlations above the critical temperature. It was shown [13] that for $0 < R < 0.5$, a disorder temperature T_D can be defined in the paramagnetic state. This temperature is determined by the temperature dependence of the spin–spin correlations along the diagonal direction. In contrast to the

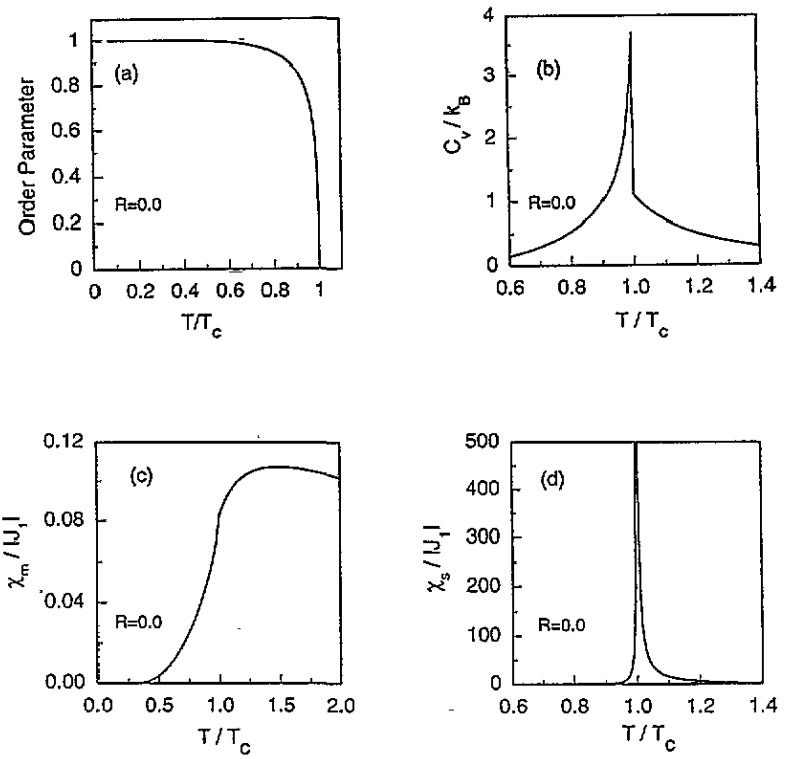

Figure 3. Temperature dependence of (a) the order parameter m (magnetization), (b) the specific heat C_v/k_B, (c) the magnetic susceptibility $\chi_m/|J_1|$, and (d) the staggered susceptibility $\chi_s/|J_1|$ for $R = 0$.

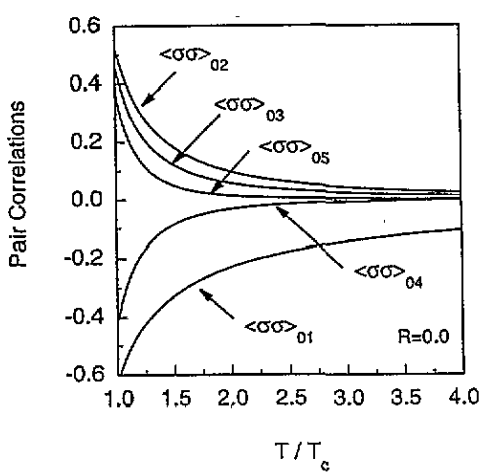

Figure 4. Temperature dependence of the spin–spin correlation function $\langle\sigma\sigma\rangle_{0j}$ for $j = 1, ..., 5$ (see figure 1), and $R = 0$.

case of $R = 0$, and due to the antiferromagnetic coupling between second neighbours, the

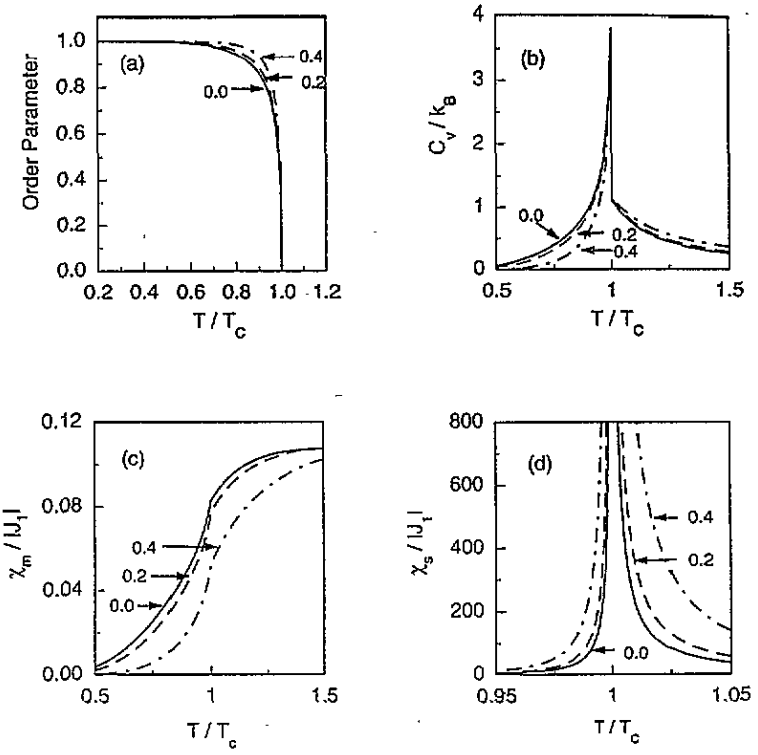

Figure 5. Temperature dependence of (a) the order parameter m (magnetization), (b) the specific heat C_v/k_B, (c) the magnetic susceptibility $\chi_m/|J_1|$, and (d) the staggered susceptibility $\chi_s/|J_1|$ for R= 0.0, 0.2, and 0.4.

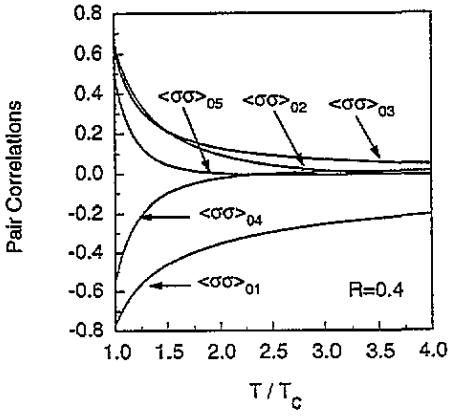

Figure 6. Temperature dependence of the spin–spin correlation function $\langle\sigma\sigma\rangle_{0j}$ for $j = 1, ..., 5$ (see figure 1), and $R = 0.4$.

ferromagnetic short-range order in the diagonal direction changes sign at temperatures above T_c. The temperature $T_{d(n)}$ at which the nth-neighbour pair correlation along the diagonal changes sign depends on the spin separation. It is observed that $T_{d(1)} > T_{d(2)} > \cdots > T_D$.

This behaviour is illustrated in figure 6, where the temperature dependence of the $\langle\sigma\sigma\rangle_{0j}$ for $j = 1, ..., 5$, and $R = 0.4$, is shown. From the five spin–spin correlations only those among first and third neighbours do not change sign. In figure 7 we show, in an enlarged scale, the results for $\langle\sigma\sigma\rangle_{0j}$ with $j = 2, 4, 5$, in the temperature range where the spin–spin correlations change sign. Note that, in addition to the diagonal correlations, the correlation between off-diagonal neighbours (fourth) also changes from antiferromagnetic to ferromagnetic. We call that temperature $T_{od(n)}$. The temperature T_D is defined as the limit of $T_{d(n)}$ for large n. Although we can only calculate three terms in the $T_{d(n)}$ series, the trend towards a limit T_D can be seen the inset to figure 7, which shows the disordering temperature along diagonal and non-diagonal directions (in units of the lattice constant).

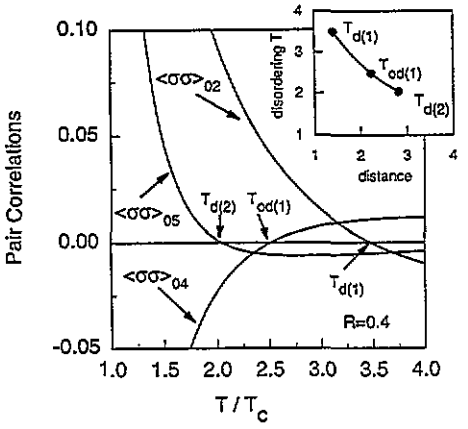

Figure 7. *Temperature dependence of the spin–spin correlation function* $\langle\sigma\sigma\rangle_{0j}$ *for* $j = 2, 4, 5$ (see figure 1), and $R = 0.4$, in the range of temperatures where a change of sign takes place. The inset shows the separation dependence of the disordering temperatures.

3.3. The paramagnetic state at $R = 0.5$

Due to the degeneracy of the ground state the system remains disordered at all finite temperatures for $R = 0.5$. A recent domain wall analysis [11] in the neighbourhood of this point indicates that the system behaves as a one-dimensional Ising chain. Our results in the nine-point approximation for C_v, χ_m, and the inverse of the staggered susceptibilities of the SAF and the AF states are shown in figure 8(a). The magnetic susceptibility is a very smooth function of T and becomes essentially zero for temperatures below $k_BT/|J_1| \sim 0.25$. On the other hand, the staggered susceptibilities diverge at $T = 0$. The specific heat has negligible values up to $k_BT/|J_1| \sim 0.17$ and then increases up to a maximum of $0.4359k_B$ at $k_BT/|J_1| \sim 0.54$.

These properties are very similar to those of the Ising chain [20]. Our results for the specific heat of the square lattice are compared in figure 8(b) with the specific heat of the one-dimensional Ising chain (dashed line), given by

$$C = \frac{J^2}{k_BT^2}\operatorname{sech}^2\frac{J}{k_BT}. \tag{5}$$

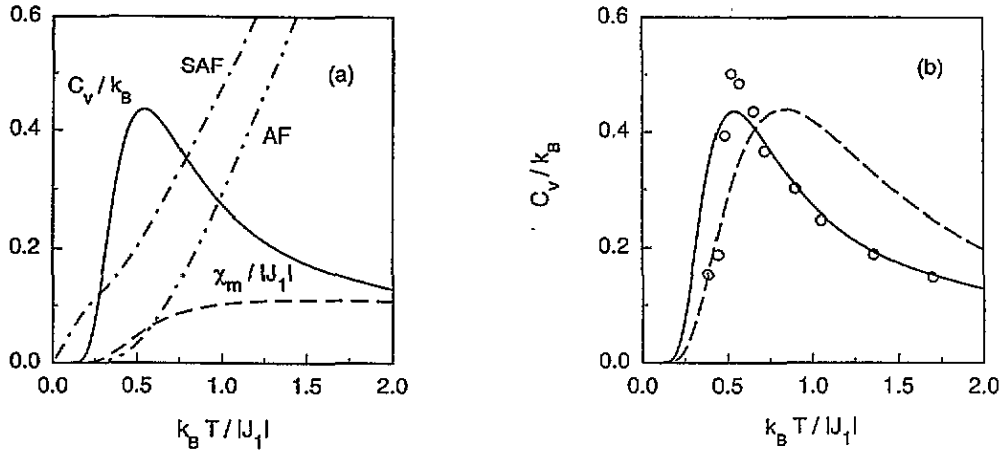

Figure 8. Results for the system with $R = 0.5$. (a) The temperature dependence of the specific heat C_v/k_B, the magnetic susceptibility $\chi_m/|J_1|$, and the inverse staggered susceptibility $|J_1|/\chi_s$ for the antiferromagnetic (AF) and superantiferromagnetic (SAF) states. (b) The temperature dependence of the specific heat C_v: the present results are given by the solid line; the Monte Carlo results [8] are denoted by o; the exact solution for the one-dimensional Ising model is shown by the dashed line.

where J is the coupling constant in the linear chain. The maximum of the specific heat occurs at the temperature T_M given by the solution of the equation

$$\tanh \frac{J}{k_B T_M} = \frac{k_B T_M}{J}. \tag{6}$$

We note that our results for the onset, the maximum value, and the general shape of C_v agree very well with the linear chain, but the temperature at which the maximum occurs is lower in our case. Since the solution of (6) is $k_B T_M = 0.8335J$, it seems that the two-dimensional Ising system with $R = 0.5$ behaves as a linear Ising chain with an effective coupling constant of $J = 0.6478|J_1|$.

We plotted also the results obtained by Monte Carlo simulations (open circles) [6]. One can further see that our results and those obtained by Monte Carlo simulations agree very well over a wide range of temperatures. A disagreement is noticeable only below $k_B T/|J_1| = 0.75$. The maximum of the specific heat obtained by MC is about 13% higher than the values predicted by the CVM.

As mentioned, there were also some speculations about the existence of a multicritical point at finite T at which the ordered critical lines for the AF and SAF states would merge. This was ruled out by exact calculations of a disorder line for values of $R < 0.5$ [12]. Our results are in agreement with such behaviour.

3.4. The superantiferromagnetic state $R > 0.5$

For values of the interaction ratio above 0.5, the degeneracy is lifted and the ground state is the collinear or superantiferromagnetic state. Now the antiferromagnetic second neighbour interaction overcomes the one among the first neighbours and produces an ordered state, that compared to the AF or F phases, has a lower symmetry; i.e. the first-, fourth-, sixth-, etc neighbour sites are no longer all equivalent. This difference in symmetry produces a different behaviour above and below $R = 0.5$.

As reported previously [9], the phase transition between the paramagnetic and the SAF states was found to be of first order for a range of interactions $0.5 < R < R_c$. Beyond the critical value R_c, the mean-field transition is second order, displaying the expected Ising-like divergence of the staggered susceptibility. Furthermore, this behaviour was consistently observed for all cluster approximations investigated here. In the particular case of the nine-point approximation $R_c = 1.144$.

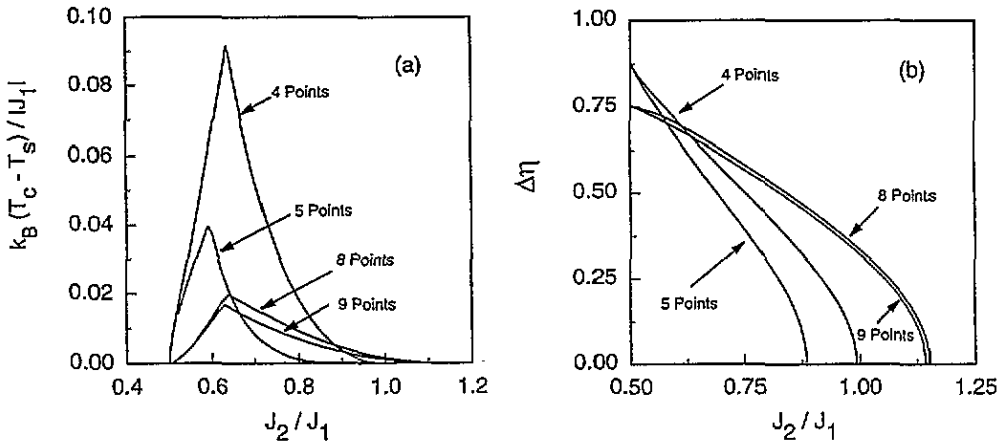

Figure 9. (a) The difference between the first-order phase transition and the instability temperatures as a function of the interactions, as obtained in the four-, five-, eight-, and nine-point cluster approximations. (b) The discontinuity of the order parameter at T_c as a function of the interactions in the various approximations used.

In view of this unexpected behaviour, we conducted a detailed analysis of the instability, or critical temperature, which is predicted by mean field to occur below the first-order transition. This critical line, or spinodal, corresponds to a metastability limit of the paramagnetic phase, below which the paramagnetic state is unstable. In Ising systems, this *mean-field* instability is with respect to fluctuations in the magnetic field, possibly staggered, and is marked by a divergence of the corresponding magnetic susceptibility. The difference between the first-order transition temperature and the highest instability temperature of the paramagnetic state is shown in figure 9(a) for the various approximations. As expected, this difference becomes smaller as the cluster approximation is improved and should, in the exact limit, coincide with the line of first-order transitions. Another unexpected behaviour of the mean-field approximation is observed near $R_0 \approx 0.60$–0.65, at which the temperature difference in figure 9(a) shows a cusp. This cusp corresponds to a change, or crossover, in the instability mode of the paramagnetic phase. For values of $R > R_0$, the instability is with respect to fluctuations in the magnetic field and the corresponding staggered susceptibility diverges, as expected of Ising systems. However, for $0.5 < R < R_0$ the instability is with respect to temperature fluctuations and the divergence takes place in the specific heat.

The first-order nature of the transition is best seen through the discontinuity of the magnetization at T_c, as shown in figure 9(b). As seen in the figure, close to $R = 0.5$ the order parameter jumps from values as high as 0.75 to zero. It is also apparent from figure 9(b) that the discontinuity of the order parameter does not behave in a systematic manner as the

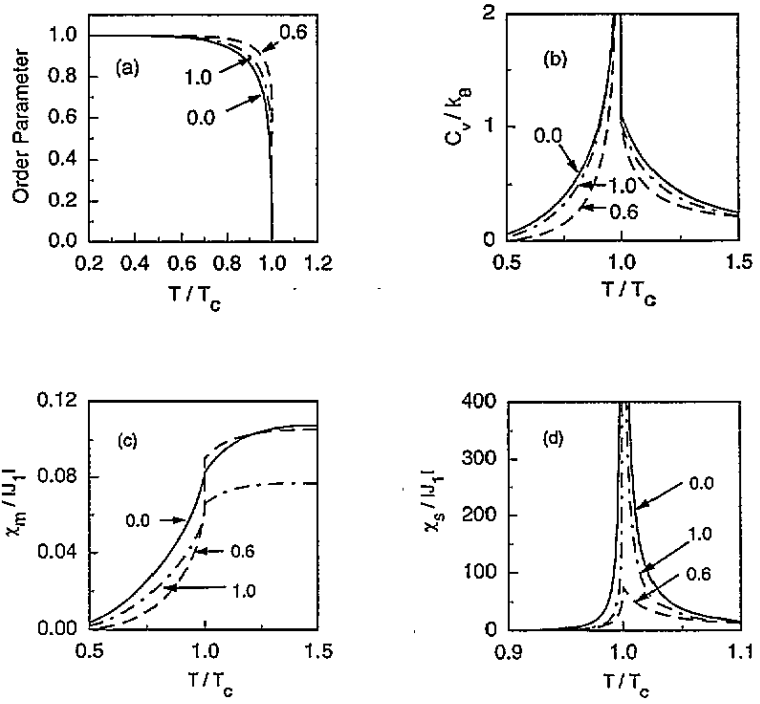

Figure 10. Temperature dependence of (a) the order parameter m (magnetization), (b) the specific heat C_v/k_B, (c) the magnetic susceptibility $\chi_m/|J_1|$, and (d) the staggered susceptibility $\chi_s/|J_1|$ for $R = 0.0$, 0.6, and 1.0.

cluster approximation changes. Thus, our results preclude the use of extrapolation schemes in order to infer the presumably exact behaviour in the limit of large clusters. As mentioned in section 1, other extrapolation schemes, such as the coherent anomaly method (CAM), can be used to investigate critical behaviour in the exact limit and to estimate critical exponents [10]. However, the straightforward application of the CAM is not warranted in view of the first-order nature of the mean-field transition as well as the instability crossover discussed above. Assuming that the first-order transition becomes second order in the exact limit, the instability crossover predicted by our mean field results suggests two distinct sets of critical exponents, rather than the continuous change observed both by Monte Carlo and the CAM analysis based on a simplified version of the CVM [10].

We show in figure 10 the results for the order parameter (average magnetization), the specific heat C_v, the magnetic susceptibility χ_m, and the staggered susceptibility χ_s for $R = 0.6$ and 1.0. The results for $R = 0$ are also included for comparison. One can recognize the first-order transition from these figures, in which the magnetic susceptibility shows a discontinuity at T_c.

The inequivalence of the two kinds of first- and fourth-neighbour site can be seen clearly in the temperature dependence of the spin–spin correlation. We plot in figure 11 the various spin–spin correlations for $R = 0.6$. In the ordered phase $\langle\sigma\sigma\rangle_{0i}$ and $\langle\sigma\sigma\rangle_{0i'}$ $(i = 1, 4)$, have opposite signs, and become equal in the disordered phase. For values of R close to 0.5 this is achieved through the abrupt first-order phase transition. As the internal energy increases with R the first-order phase transition becomes weaker until, at the point R_c, the transition becomes of second order.

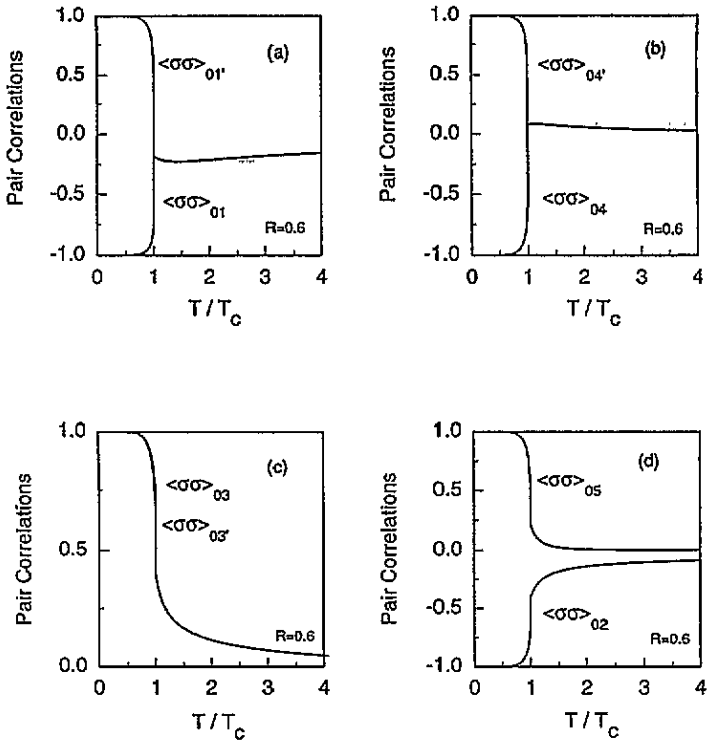

Figure 11. Temperature dependence of the spin–spin correlation function $\langle\sigma\sigma\rangle_{0j}$ for j = 1,1' (a), j = 4,4' (b), j = 3,3' (c), and j = 2,5 (d), and $R = 0.6$.

3.5. The phase diagram

We show in figure 12 the calculated phase diagram (solid line) in the T_c against R parameter space. In this figure we include for comparison the results obtained for T_c by other methods: the values obtained with Monte Carlo simulations [6–8] are marked with open circles; those marked with triangles correspond to real space renormalization group results [21]; the crosses correspond to Monte Carlo renormalization group results [5]; and the open diamonds to series expansion results. One can see the excellent agreement between our results and those of Monte Carlo and series expansion studies.

In the nine-point approximation the phase transition taking place in the range of interactions $0.5 < R < 1.144$, is of first order. In figure 12, the bicritical point is denoted by a closed circle. We recall that the instability temperature occurs immediately below the line of first-order transitions. The difference between T_c and the instability temperature in the nine-point approximation is smaller than $1.8 \times 10^{-2}|J_1|/k_B$. This cannot be resolved in the figure. The phase transitions taking place outside that range of interactions are of second order.

Although, as mentioned, the crossover between two instability temperatures suggests two distinct critical behaviours for $R > 0.5$, the existence of a weak first-order transition cannot be entirely ruled out. Thus, a possible explanation of the non-universal critical behaviour for $R > 0.5$ observed, for example, in Monte Carlo simulations, could be due to the first-order character of the phase transition.

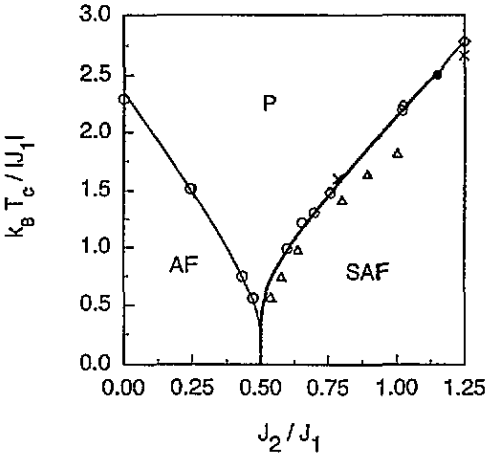

Figure 12. Dependence of the transition temperature $k_B T_c/|J_1|$ on the interaction ratio $R = J_2/J_1$. The various phases are the paramagnetic (P), the antiferromagnetic (AF), and the superantiferromagnetic (SAF). The solid lines are the present results; Monte Carlo results [6–8] are denoted by ○; real space renormalization group results [21] are denoted by △; Monte Carlo renormalization group results [5] are denoted by ×; series expansion results [4] are denoted by ◇. The phase transition in the range $0.5 < R < 1.144$ is of first order. The bicritical point is indicated by ●.

4. Summary

We have presented a detailed study of the phase transitions occurring in the square Ising antiferromagnets. The Hamiltonian contained first- and second-neighbour interactions and was solved by means of the cluster variation method in various cluster approximations. The thermodynamic properties of the model were investigated for a large range of interactions. The antiferromagnetic phase occurring for $0 < R < 0.5$ was studied in the ordered and the paramagnetic states. The disordering temperature T_D produced by the competing interactions was clearly observed through the temperature behaviour of the spin–spin correlations among the various neighbours within the nine-point cluster. Our calculation showed that the system with $R = 0.5$ behaves as a one-dimensional Ising chain. The comparison of our results with the exact temperature dependence of the specific heat led us to the conclusion that this particular case shows one-dimensional behaviour with a reduced coupling constant.

The mean-field approximation predicted that the phase transitions taking place in the range $0.5 < R \lesssim 1.2$ are of first order. This behaviour was confirmed by solving the Hamiltonian using four-, five-, eight-, and nine-point clusters as units. Furthermore, these approximations also predict a crossover in the spinodal temperatures occurring immediately below the first-order transition.

Acknowledgments

One of us (JLM-L) acknowledges the support of the Alexander von Humboldt Foundation and of the Consejo Nacional de Ciencia y Tecnología (Mexico). This work was supported in part by the National Science Foundation through grant Nos DMR-91-14646 and INT91-14645, and by Consejo Nacional de Ciencia y Tecnología through grants C90-07-0383 and 1774-E9210.

References

[1] Nightingale M P 1977 *Phys. Lett.* A **59** 468
[2] Barber M N 1979 *J. Phys. A: Math. Gen.* **12** 679
[3] Wu F Y 1971 *Phys. Rev.* B **4** 2312
[4] Oitmaa J 1981 *J. Phys. A: Math. Gen.* **14** 1159
[5] Swedensen R H and Krinsky S 1979 *Phys. Rev. Lett.* **43** 177
[6] Landau D P 1980 *Phys. Rev.* B **21** 1285
[7] Binder K and Landau D P 1980 *Phys. Rev.* B **21** 1941
[8] Landau D P and Binder K 1985 *Phys. Rev.* B **31** 5946
[9] Morán-López J L, Aguilera-Granja F and Sanchez J M 1993 *Phys. Rev.* B **48** 3519
[10] Tanaka K, Horiguchi T and Morita T 1992 *Phys. Lett.* A **165** 266
[11] Grynberg M D and Tanatar B 1992 *Phys. Rev.* B **45** 2876
[12] Blote H W J, Compagner A and Hoogland A 1987 *Physica* A **141** 375
[13] Stephenson J 1970 *Phys. Rev.* B **1** 4405
[14] Kikuchi R 1951 *Phys. Rev.* **81** 988
[15] Bragg W L and Williams E J 1934 *Proc. R. Soc.* A **145** 699
[16] Guggenheim E A 1935 *Proc. R. Soc.* A **148** 304
Bethe H A 1935 *Proc. R. Soc.* A **150** 552
Peierls R 1936 *Proc. R. Soc.* A **154** 207
[17] Kramers H A and Wannier G H 1941 *Phys. Rev.* **60** 252; 1941 *Phys. Rev.* **60** 263
[18] Morán-López J L and Sanchez J M 1993 *Physica* C **210** 401
[19] Sanchez J M, Ducastelle F and Gratias D 1984 *Physica* A **128** 334
[20] McCoy B M and Wu T T 1973 *The Two-dimensional Ising Model* (Cambridge, MA: Harvard University Press) p 40
[21] Nauenberg and Nienhuis B 1974 *Phys. Rev. Lett.* **33** 944